https://doi.org/10.22226/2410-3535-2021-4-533-543 PACS: 61.46.-w, 61.50.Ks, 62.20.Qp

Al based layered *in situ* metal-matrix composites fabricated by constrained high pressure torsion

G. F. Korznikova[†,1], E. A. Korznikova[1,2,3], G. R. Khalikova[1,3], K. S. Nazarov[1], R. Kh. Khisamov[1], S. N. Sergeev[1], R. U. Shayakhmetov[1], R. R. Mulyukov[1,3]

[†]gfkorznikova@gmail.com

[1]Institute for Metals Superplasticity Problems, RAS, Ufa, 450001, Russia
[2]Ufa State Aviation Technical University, Ufa, 450008, Russia
[3]Ufa State Petroleum Technological University, Ufa, 450062, Russia

Severe plastic deformation is often used to obtain an ultrafine-grained structure in metals and alloys, and this direction in metal processing continues to develop actively. At the same time, severe deformation also makes it possible to perform interfusion of different metals for the synthesis of ultrafine-grained and nanocrystalline materials with heterogeneous structure that determines their unique set of properties. Primarily, pure metal powders were used as starting components, and the method was called mechanical alloying. In recent years, a new approach has been developed, consisting in solid-phase connection of thin disks by means of shear deformation on Bridgman anvils, and the resulting composite materials were called hybrid composites. This paper presents the results of a study of hybrid composites based on Al processed by severe plastic deformation. Bulk hybrid composites Al-Cu, Al-Nb, Al-Mg, Al-Ti were fabricated in one step by shear deformation under high pressure. All obtained composites were monolithic with a heterogeneous structure consisting of a plastic aluminum matrix and harder inclusions of second metals and intermetallic particles. Varying the annealing temperature allows processing composites with different fractions of intermetallic particles. Analysis of microstructure, phase composition and properties has led to several unusual results. Using the Al-Cu composite as an example, a significant decrease in the activation energy for the growth of intermetallic particles during annealing was shown. In Al-Nb composite, it was revealed that the formation of a small amount of the intermetallic phase Al_3Nb occurs at room temperature, while the equilibrium temperature of formation of this phase is above 600°C. Analysis of the tensile properties of Al-Cu composites showed a significant increase in the strength compared to the initial components. The results obtained are discussed and explained in terms of the contribution of various factors to the strengthening and softening of the composite material.

Keywords: metal matrix composites, high pressure torsion, interface bonding, phase transformations, intermetallics, mechanical properties.

1. Introduction

The increased demand for materials with enhanced functional properties has arisen due to the rapid development of various technologies, which led to a huge growth of attempts in finding ways to create new composite materials that can meet the requirements associated with the overall improvement of the characteristics of existing devices. The approach allowing to take advantage from materials of different structure and sometimes of different origin has proven applicable in aerospace [1], automotive [2], electronic [3], construction [4] and other industries. Among the many different composites, aluminum-based metal matrix composites (MMC) have attracted considerable attention due to their low weight, high specific strength, hardness and corrosion resistance [5–7]. The numerous production methods for MMC include spray forming, squeeze or stir casting, and powder metallurgy methods [5]. Like alloying, in many cases the hardening effect in aluminum-based composites is associated with the formation of an intermetallic phase [8–11]. For example, it was revealed that in cast Al-Cu and Al-Si-Cu alloys, the key strengthening precipitates are disc-shaped precipitates of the tetragonal Θ' Al_2Cu phase [10]. Annealing at 200°C results in Al_2Cu phase deterioration over time leading to the formation of Θ phase precipitates with incoherent interfaces with the Al matrix, improving the thermal stability of the alloy. At the same time, the amount of the hardening precipitates in cast alloys is limited mainly by the ultimate solubility of metals. In case of composite materials, revealing the strengthening mechanisms is more complicated because of the presence of numerous factors, such as contaminations and consolidation-induced lattice defects contributing to the complex of mechanical properties of the material. A lot of research has been done. in this area, and among all existing methods of metal matrix composite fabrication, various deformation techniques were found to be quite beneficial in this respect because of the ability to combine several types of strengthening mechanisms, e. g., explosive welding, diffusion bonding, vacuum hot pressing and accumulative roll bonding. [5, 6, 8, 11] The major factor for successfully manufacturing metal-matrix composites by direct bonding of dissimilar materials is achieving homogeneous interface

bonding while their properties are controlled by the size, morphology and volume fraction of the reinforcements as well as the nature of the matrix-reinforcement interfaces [7,12].

Approaches involving deformation methods of composite fabrication can be considered profitable for several reasons including strain-induced defect strengthening [13–16] and enhanced diffusivity of components due to the presence of a high concentration of point defects associated with large strains [12,17,18].

Considering the abovementioned facts, severe plastic deformation can be regarded as the most promising technique in terms of producing true bulk nanostructures with the highest shear strains in the material without fracture and the highest volume fraction of point and line defects alongside with grain boundaries which are characterized by high angles of misorientation [19]. Details of HPT treatment are addressed in [20,21]. One of the most important issues is the radial dependence of shear strain which leads to inhomogeneity both in the microstructure and in the hardness values being dependent on the distance from the center and theoretically zero at the center of the disc.

Generally, HPT-processed metals and alloys show a significant enhancement of the mechanical properties, especially hardness and strength, in comparison with their coarse-grained counterparts due to exceptional grain refinement. However, due to the small size of the disks, the mechanical properties were estimated mainly by measurements of microhardness and nanoindentation.

Initially HPT was performed on pure metals [19], later it was used for alloys and metallic powders [22,23], and then for the mechanical bonding of bulk dissimilar metals [24–33], where HPT induces plastic flows of the material interfaces and their gradual transformation in well-bonded zones [24]. Moreover, this method allows obtaining in one step at room temperature a number of compounds of sufficient size to certify the structure as well as physical and mechanical properties for a relatively short time The output was termed HPT hybrid [26].

Due to specific stress-strain state assisting the mechanical alloying of components, this method has been successfully applied for fabrication of homogeneous composite materials numerous combination of metals, for instance, in Al-Cu [18,29–31], Al-Mg [13,14], Al-Ti [27], Cu/steel [32], Zn-Mg [27,28] and many other systems, including combinations with carbon nanopolymorphs [33] which allow to improve the properties of the final composite due to remarkable properties of this new generation materials.

In particular, this approach has been applied to light metals and alloys to expand their upper limits of mechanical properties, such as strength and ductility, while maintaining the alloy density during grain refinement and the simultaneous solid-state reaction during HPT. Considerable attention has been intended on aluminum-based metal-metal composites due to their high specific strength, hardness, wear resistance and fatigue strength. This report provides an overview of our recent research of metal matrix composites fabricated by application of HPT on Al-Cu, Al-Mg, Al-Nb and Al-Ti alloy systems and the evolution of microstructure phase content and mechanical properties determined from direct tensile experiments of the synthesized alloy systems.

2. Materials and Methods

2.1. Sample preparation

As starting materials for research, we used aluminum with a purity of 99.5 wt.%, copper (99.90 wt.%) niobium (99 wt.%), titanium (99.2 wt.%) and magnesium (95 wt.%) with coarse grained structure in the shape of disks with 0.5 mm thickness and 12 mm in diameter. HPT processing was applied to four different metal systems namely Al-Cu, Al-Mg, Al-Nb and Al-Ti systems. Constrained HPT processing [19] was applied to a set of 3 disks with the alternation of layers, i. e. plate of hard phase metals were placed between two plates of soft Al. As an example, Fig. 1a shows the set of Al-Cu-Al discs. Thus, the total thickness of the samples before deformation was 1.5 mm. The anvils with a diameter 12 mm and grooves with a total depth 0.5 mm were used for constrained HPT. The set was placed between the anvils, pressed to 6 GPa and processed at room temperature, with a rotation speed of 1 rotation per minute. The total number of anvil revolutions (N) varied from 10 to 30. Final thickness of the processed samples was about 1 mm (Fig. 1b).

To obtain composites with inclusions of intermetallic phases, annealing was performed. Annealing temperatures for each composite were selected based on DSC measurements, and phase composition was checked by X-ray diffraction phase analysis before and after annealing.

X-ray diffraction analysis was performed at the cross-section of the disk a high-resolution Rigaku Ultima IV X-ray diffraction system using a Cu-K_α radiation. Phases content was quantified by means of Rietveld analysis.

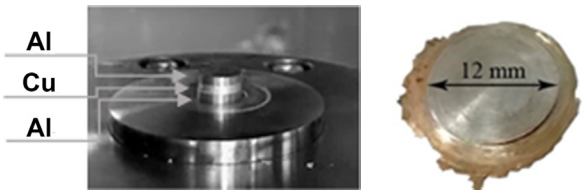

a b

Fig. 1. (Color online) Set of three discs (Al-Cu-Al) before HPT (a), general view of as processed sample after HPT (b).

2.2. Microstructure characterization

The samples for microstructural characterization were cut vertically along discs diameter and prepared using conventional metallographic techniques followed by polishing with colloidal silica suspension. Microstructure analysis was conducted using scanning electron microscope Tescan Mira 3LMH with back scattered electron (BSE) detectors at accelerating voltage 20 kV. The chemical composition of samples was investigated using scanning electron microscope Tescan VEGA 3 SBH with an energy dispersive X-ray spectroscopy (EDS) attachment. Transmission electron microscopy studies were performed on the JEM 2100 Plus microscope at accelerating voltage of 200 kV. Selected area diffraction pattern was taken from the area 2 μm^2.

2.3. Mechanical testing

Microhardness was measured by the Vickers method on an AFFRI DM8A microhardness tester with the indentation load 10 g.

Two specimens for conducting tensile strength tests were cut from the disc from the middle radius zone. The scheme of the disc cutting and microstructure in the working area of the tensile samples are shown in Fig. 2 a. Tensile tests were carried out using specially elaborated locks (Fig. 2 b.) mounted in an Instron Model 1185 tensile testing machine. The tests were carried out at a tensile speed of 1 mm/min until fracture of the sample. The ductility of the composites due to the small working base of the samples was not evaluated.

3. Results and discussions

3.1. Microstructure evolution and phase transformations

Fig. 3 presents scanning electron microscope micrographs showing low magnification overview of composites cross-section after HPT in the as processed state. The dark areas on the scanning electron microscope images correspond to the Al-rich phase in Al-Cu, Al-Nb and Al-Ti composites, while in Al-Mg composite Al-rich phase corresponds the bright areas. All sample are monolithic, and no pores are observed. However, the degree of mixing is different in different composites. Al-Cu and Al-Mg hybrids were processed with 10 and 20 revolutions of anvil, while for the formation of an Al-Nb hybrid with good mixing, it is necessary to increase the number of revolutions to 30 [34]. The smallest mixing occurred in Al-Ti composite where significant fragmentation of the titanium layers and their mixing with aluminum did not occur. An increase in the number of revolutions to 30 did not lead to significantly better mixing of the components in Al-Ti composite. This means that the Al-Ti composite needs more pressure to be applied.

The detailed microstructure SEM observation at higher magnification revealed a complex layered microstructure developed in the rest composites. The originally flat interface between Al and second metal layers transforms and some bending and vortices-like folding are formed. The formation of vortices is a result of instabilities of interfaces between dissimilar metals caused by local blocking of shear deformation as it has been discussed recently [35,36].

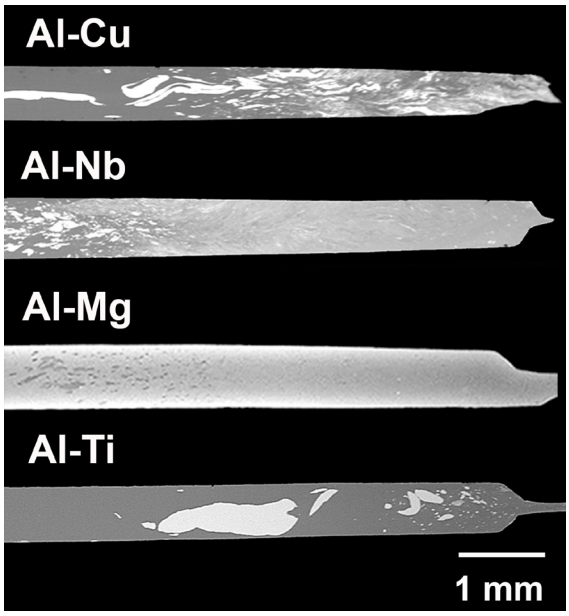

Fig. 3. Back scattered electron image of the composites in the as-processed state: Al-Cu hybrid produced by at the $N=10$, Al-Nb hybrid produced by at the $N=30$, Al-Mg hybrid produced by at the $N=20$, Al-Ti hybrid produced by at the $N=30$.

Depending on the distance from the center of the sample, mixing of the components in Al-Cu, Al-Nb and Al-Mg composites is different (Fig. 3). The central part has three clear layers and look very similar to the initial layered structure, but the layers are much thinner than in the original sample before HPT. In the mid-radius area, intermediate layer is no longer uniform. Some fine elongated fractions of the second metal in the Al matrix appear. Close to the edge, lamella-type areas become much thinner and longer, which is caused by a strain increase when moving from the center towards the periphery. It can be seen that very thin layers of less than 5 μm thickness embedded in Al and form submicron multilayer structure. Thus two-component aluminum-matrix composites Al-Cu, Al-Nb, Al-Mg, with a gradient distribution of structural elements were obtained. It was found that Al-Ti composition needs changing the conditions of deformation, foremost increase the applied pressure and/or significant increase of number of anvil revolutions, what allows to vary the parameters of the composite structure (Fig. 3).

More detailed microstructure study of the peripheral area of the composites in as-fabricated state was carried out by means

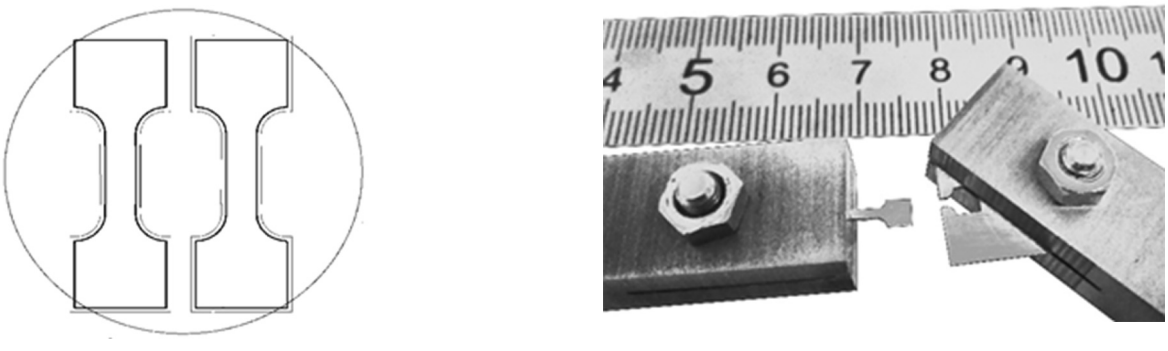

a b

Fig. 2. Scheme of tensile specimens cutting from a disc (a), tensile testing accessories (b).

of transmission electron microscope at high magnifications. An ultrafine-grained structure with equiaxed grains of about 200-300 nm in size with low dislocation density was revealed in Al layers of Al-Cu composite (Fig. 4a). The grain boundaries are straight and have banded contrast, indicating that dynamic recrystallization occurred in the aluminum phase of the composite during HPT. Individual nanoscale nucleation of the Al_2Cu intermetallic phase indicated by arrows appear in the nanograined structure. It should be noted that no precipitations were observed in mid-radius area. A more noticeable refinement occurred at the periphery of Al-Nb composite, where grain size reduced to 30 nm (Fig. 4b). On the selected area diffraction patterns, along with rings corresponding Al and Cu (Nb), reflections with large interplanar spacings corresponding to the Al_2Cu (Al_3Nb) phase are visible as a circles closest to transmitting beam.

The detailed analysis of phase composition and its evolution upon annealing by X-ray diffraction and energy dispersive X-ray spectroscopy studies of Al-Cu and Al-Nb hybrids were reported earlier [20, 21]. The most important results are following. Severe plastic deformation by HPT is able to promote solid-state reactions with intermetallic phases generation at room temperature due to the fact that material during high pressure torsion is in a state far from equilibrium. An increase in the degree of deformation with increasing distance from the center leads to a gradient type change in the phase composition in as-processed samples. In the central region, where the degree of deformation is minimal, mixing of the components did not occur, as well as the formation of the intermetallic phase. In the mid-radius part where the degree of deformation and the density of the phase boundaries are substantially greater, separate layers and particles of the intermetallic phase appeared in the nanolaminated structure. As the distance from the center increases, the fraction of such intermetallic compounds increases. Thus, HPT induced the nucleation of the intermetallic compound, which is identified mainly on the periphery of the composite disc formation of intermetallic phase was observed in Al-Nb and Al-Cu composites in the as-processed state and is not detected in Al-Mg and Al-Ti hybrids.

However, both Al-Nb and Al-Cu metallic systems supports several intermetallic phases and in as-processed state revealed here formation of only one intermetallic phase — Al_3Nb (≈3%) in Al-Nb composite, and Al_2Cu (≈0.5%) in Al-Cu composite. This is not a trivial fact worth discussion and explanation. Similar effect was observed after mechanical alloying [37] in and friction stir welding [38] where authors report the decrease of the Al_3Nb phase formation temperature from 933°C to 454°C. Explanation of the single intermetallic phase formation instead of three present, for example, in Al-Nb phase diagram could be the following: (i) in [37] it was shown that the effective heat of formation in Nb_3Al, Nb_2Al and Al_3Nb decreases as listed above and according to that, Al_3Nb is the first phase formed in the interface and (ii) due to quite limited solubility of Nb in Al, this phase has favorable conditions of formation due to lowest demand of Nb associated with the intermetallic formation. The latter is because the growth of the intermetallic composite takes place on the Al_3Nb/Al surface as a result of exothermic reaction between the matrix and intermetallic particles and this process can continue only in case if the change in Gibbs free energy is negative. Since the change of free energy in solid media is equal to the enthalpy [38], one can connect it with the heat released for one mole of present atoms (Al) is influenced by the effective concentration of limiting element (Nb) in the composition which is called effective heat of formation, being the highest for the Al_3Nb phase. These arguments are also supported by the XRD data [45].

3.2. Annealing induced phase transformations

Annealing induces additional phase transformations and permits the synthesis of intermetallic reinforced metal-matrix composites. As an example, Al-Cu and Al-Nb hybrids are described below.

Annealing temperatures are selected on the basis of differential scanning calorimetry (DSC) measurements, which showed for Al-Cu composite the presence of a broad peak in the temperature range 150 – 450°C. X-ray phase analysis of the composite immediately after deformation, along with Al and Cu, revealed 0.5% of the Al_2Cu phase. After annealing alongside with Al_2Cu phase AlCu and Cu_9Al_4 intermetallic compounds were detected. As expected, formation of the maximum fraction of Al_2Cu, AlCu, Cu_9Al_4 intermetallic compounds occurred after annealing at 450°C — the temperature of phase transformations termination according to the DSC curve. The total fraction of intermetallic compounds in the composite after annealing at 450°C for 30 minutes reached 49.5%.

X-ray phase analysis after isothermal annealing at lower temperatures 150, 170, 190, and 210°C allowed to analyze the

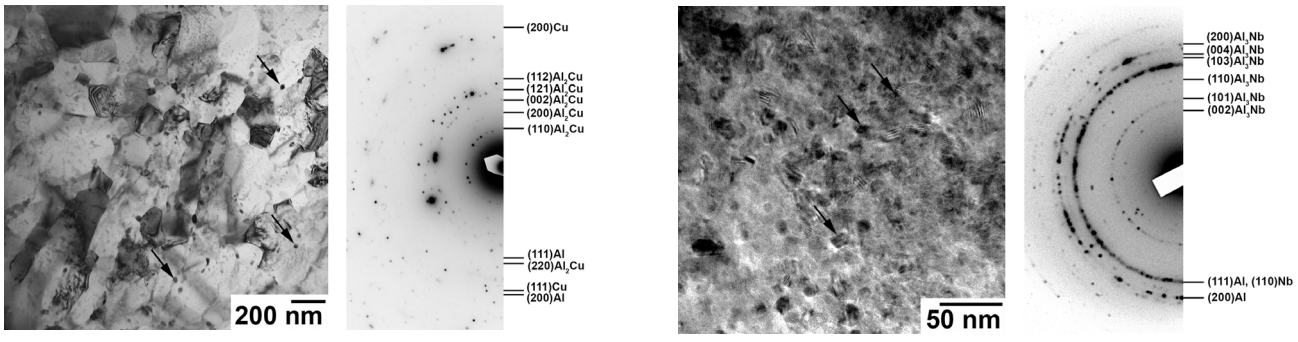

a b

Fig. 4. Transmission electron microscope bright field image and selected area diffraction patterns of an Al-Cu (a) and Al-Nb (b) composites in the as-fabricated state in the peripheral area.

kinetics of phase transformations and to evaluate the activation energy for the growth of Al_2Cu phase being equal to 0.48 eV, which is significantly lower than that of bulk diffusion of Cu in polycrystalline Al. Analysis of the kinetics of the formation of intermetallic phases indicates that bulk diffusion is the main mechanism of intermetallic compounds growth [30].

The microstructure and EDS data in different parts of the Al-Cu sample in as-processed state and after annealing at 450°C for 30 minutes are presented in Fig. 5. In addition to dark areas corresponding to Al and white areas corresponding to Cu, dark gray, gray, and light gray layers are detected. EDS for individual points showed that the observed zones correspond to Al_2Cu, AlCu and Al_4Cu_9. The maximum proportion of IMC is observed at the peripheral area, which is associated with maximum shear deformation at the edges and, consequently, with the formation of a high-defect ultrafine grained structure, which provides the best conditions for mixing the components.

Examples of the indexed X ray diffraction patterns of the Al-Nb composite sample in as processed state (a) and after annealing at 400°C and 600°C are presented in Fig. 6.

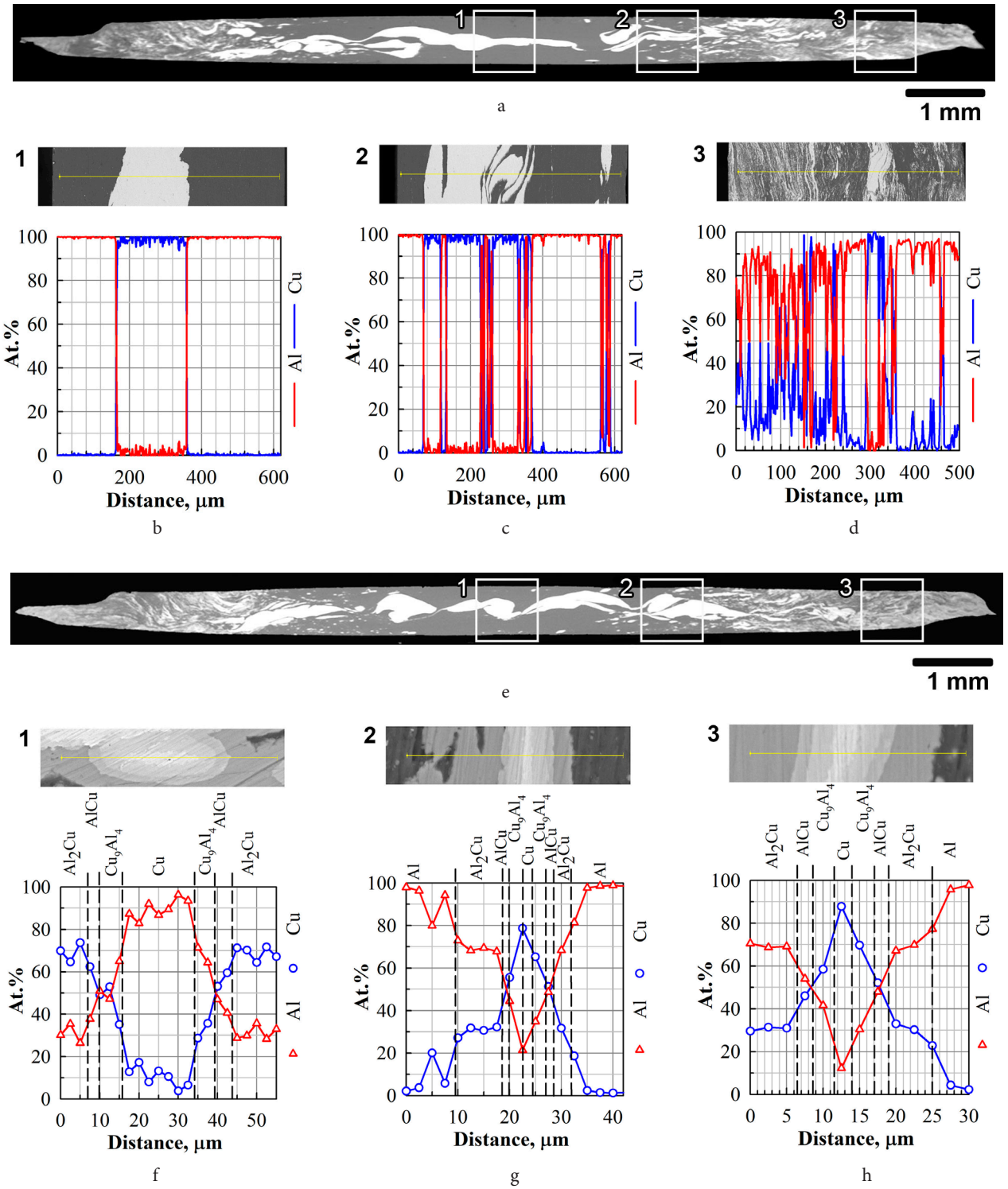

Fig. 5. (Color online) Back scattered electron image of the of the Al-Cu hybrid in the as-processed state (a) and after annealing (e). EDS analysis for Cu and Al, in the center (1) (b, f), at midradius (2) (c, g) and in the periphery (3) (d, h) for as-processed (b – d) and annealed (f – h) samples.

The HPT-deformed samples are primarily composed of crystalline fcc Al and bcc Nb along with small volume fraction of tetragonal intermetallic Al_3Nb phase. Analysis of annealing induced phase composition evolution reveals the increase of the Al_3Nb fraction with the appropriate decrease of pristine elements.

The dynamics of the intermetallic phase growth strongly depends on the annealing temperature and at 600°C the fraction of Al_3Nb surpasses that of pure Nb already after 1 minute of annealing while for 400°C this switch happens after more than half an hour. The final amount of the Al_3Nb also increases upon the annealing temperature and makes 15% and 27% after 51 min annealing at 400°C and 600°C respectively.

The microstructure and EDS data in different parts of the Al-Nb hybrid in as-processed state and after annealing at 600°C for 30 minutes are presented in Fig. 7. By contrast to Al-Cu composite on the edge of the Al-Nb disk sample the

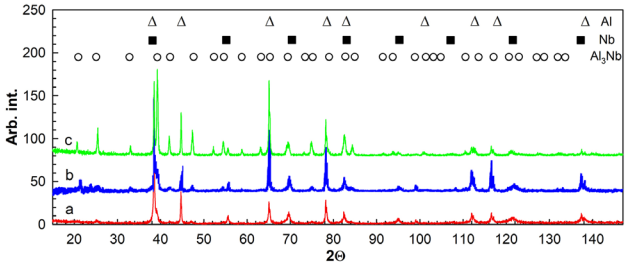

Fig. 6. (Color online) X ray diffraction patterns of the Al-Nb composite sample in as processed state (a) and after annealing at 400°C (b) and 600°C (c) during 30 minutes [33].

element distribution is rather homogenous. Al/Nb ratio on the edge is about 4/1. The closest in composition of known intermetallic compounds of the equilibrium Al-Nb system is Al_3Nb intermetallic compound. So, the microstructure on the edge consists mainly of Al_3Nb phase with some inclusions of Al enriched areas.

3.3. Microhardness distribution and evolution upon annealing

Microhardness distribution in HPT processed Al-Cu, Al-Mg, Al-Nb and Al-Ti hybrids is shown in Fig. 8. Generally, the microhardness increases with distance from the center and reaches maximum values near the sample periphery. The exception is Al-Ti hybrids, where, under the used pressure of HPT, the mixing of the components turned out to be poor. Gradient distribution of microhardness in Al-Cu, Al-Mg, Al-Nb hybrids is apparently associated with a greater degree of deformation and accordingly with greater hardening at the sample edge. Previously this type of behavior was reported for pure metals and alloys [19] and later for HPT processed metal-matrix hybrids [25, 26]. After annealing certain decrease in the HV of the aluminum matrix, which is especially clearly seen in the center of the hybrids is obviously the consequence of annealing driven recrystallization. Overall, the structure obtained in Al-Cu, Al-Mg, Al-Nb composites after annealing can be characterized as heterogeneous, consisting of a ductile aluminum matrix and hard inclusions of intermetallic compounds with a gradient increase in microhardness from the center to the edge of the sample.

Analysis of the microhardness distribution in Al-Nb hybrid shows that the latter does not follow the most common path of the increase of the microhardness upon the increase of the distance from the center. However, in Al-Nb composite the maximal microhardness value (≈300 HV) is revealed to locate in the middle radius part, demonstrating almost a twice smaller value at sample edges. The lowest microhardness (about 100 HV) is observed in the center of the sample. Annealing at 400°C lead to redistribution of HV values to a common for HPT processed samples V-profile.

In order to understand this unconventional microhardness behavior, one should analyze the possible contributions to hardening of the material originating from different factors. The major factors determining the mechanical behavior of the material are (i) accumulation of strain induced defects, (ii) amount of interphase areas formed during the amalgamation of dissimilar metals and (iii) amount of hard intermetallic phases.

In the as deformed state only first two factors matter since the fraction of Al_3Nb phase is very low. Thus, in the central part of the sample according to microstructure analysis the coarse fragments of Al and Nb phases are detected defining the low microhardness in this region. In the area of the $R/2$ one can observe the nanolaminated structure with enhanced area of interphases which in combination with high density of defects contribute strongly to the HV sharp growth. Finally, at the sample edge the maximal degree of shear deformation results in the formation of the strain induced solid solution, that results in the decrease of interface hardening component which is obviously not compensated by the solid solution hardening.

Annealing of the deformed composite at 400°C results in the overall decrease of the microhardness due to annealing of HPT induced defects. However, the values of the microhardness are increased on the edge of the sample after annealing due to formation of the Al_3Nb being the result of the enhanced diffusion in the solid solution region.

3.4. Tensile tests

Table 1 presents the ultimate tensile strength of composites in the as-processed state and after annealing.

Generally the yield strength of sandwich sheet metals should follow the rule of mixture [39], which is an average of component yield strengths weighted by volume fractions and expressed as:

$$\sigma = \sum V_i \sigma_i, \qquad (1)$$

where V_i and σ_i are the volume fraction and the flow properties of component i, respectively. Therefore, tensile tests were carried out on the initial components in the coarse-grained state and after the HPT processing under the same deformation conditions. Table 2 shows the values of ultimate tensile strength of pure Cu, Nb, Mg, Ti in the annealed and HPT processed states.

Tensile test demonstrated that HPT processed Al-Cu composite exhibits strengthening that much higher than the

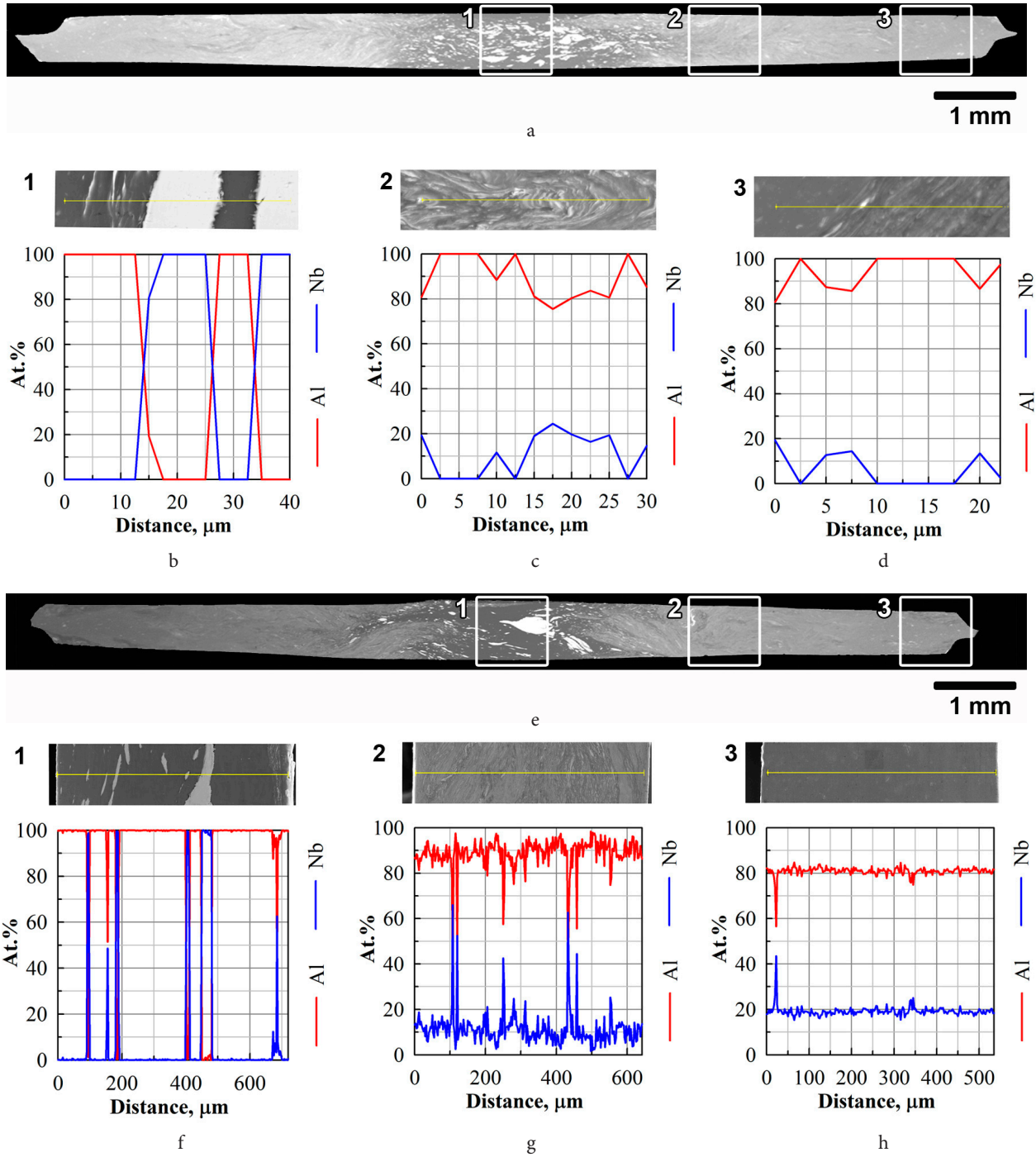

Fig. 7. (Color online) Back scattered electron image of the Al-Nb composite sample in the as-processed state (a, b, c, d) and after annealing (e, f, g, h) microstructure details in the center (b, f), at mid-radius (c, g), at the peripheral area (d, h) and elemental distribution along the line depicted at the top of the panel in the form of relative intensities plot with relation to the scanning distance for Nb and Al, marked by the blue color and the red color, respectively.

result predicted the rule of mixture. It suggested that an extra strengthening mechanism existed in the HPT-processed multilayered composite. Recent reports on heterogeneous layered structures [40] highlighted this mechanism, which referred to hetero-deformation induced back stress strengthening [41–43]. Detailed analysis of mechanical behavior of Al-Cu composite are provided in [21].

Subsequent annealing of the Al-Cu composite at 150°C led to a decrease of dislocation density and reduction of strain gradients that provides degradation of back-stress hardening in transition areas. So the recovery process leads to a noticeable decrease in strength. Further increase in the annealing temperature to 450°C led to an even more significant tensile strength reduction (Table 1).

By contrast Al-Nb, Al-Mg and Al-Ti composites demonstrate ultimate strength even lower than initial components (Nb, Mg, Ti) subjected to HPT. The key role in the tension of the samples is apparently played by the compatibility of the deformation of the composite components. Despite the fact that after quasi-hydrostatic torsion under high pressure the composite disks of the Al-Nb, Al-Mg, and Al-Ti composites have no visible pores and cracks, cracks appear during tension,

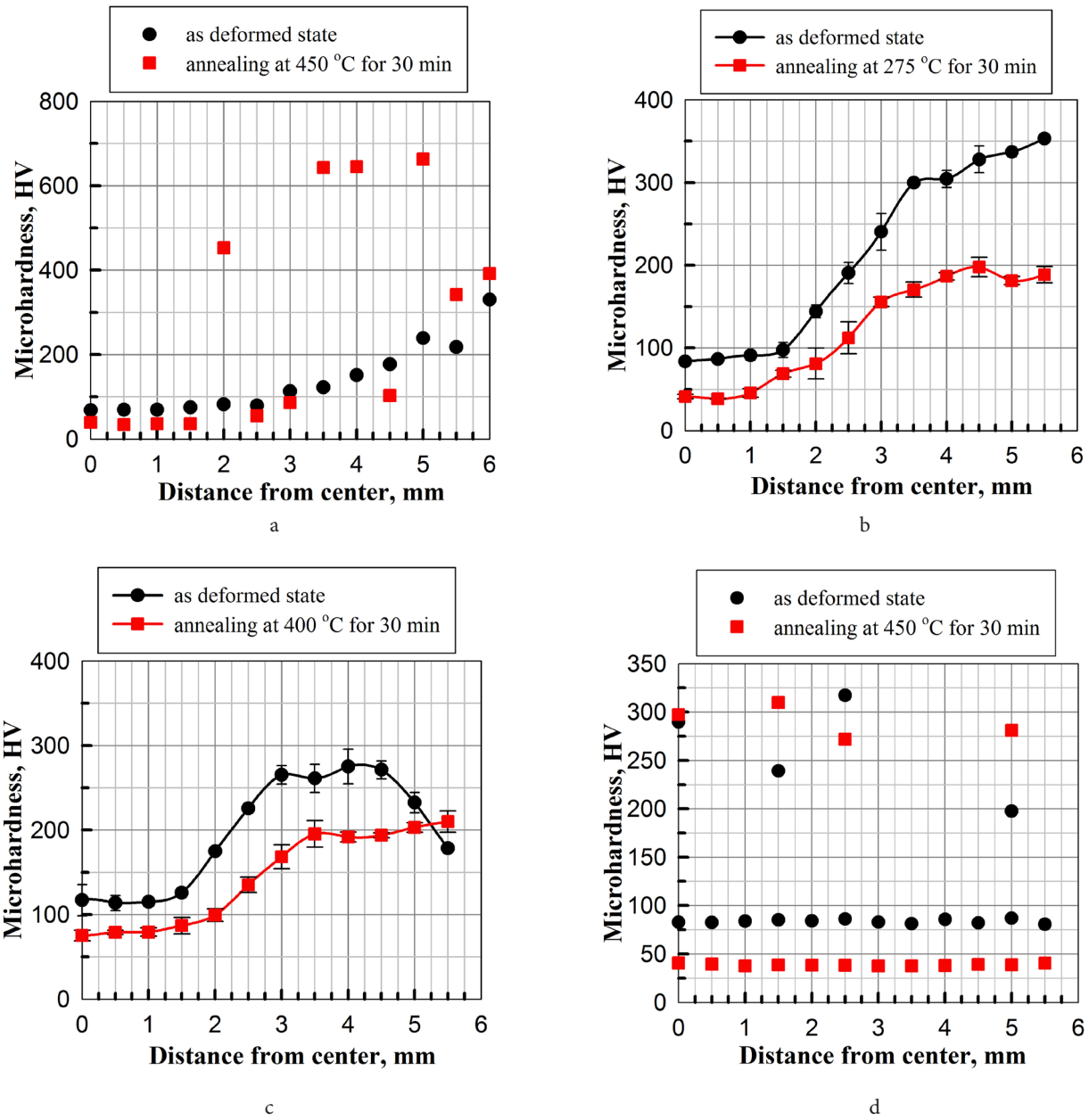

Fig. 8. (Color online) Microhardness distribution over the cross section of the Al-Cu (a), Al-Mg (b), Al-Nb (c), Al-Ti (d) hybrids in the as-processed (black line), after annealing (red line).

Table 1. Ultimate tensile strength of composites in the HPT-processed state and after subsequent annealing.

Composite type	Additional thermal treatment	Tensile strength σ_t, MPa
Al-Cu HPT	-	485
Al-Cu HPT	150°C 30 min	320
Al-Cu HPT	350°C 30 min	167
Al-Nb HPT	-	177
Al-Nb HPT	400°C 30 min	337
Al-Nb HPT	600°C 30 min	290
Al-Mg HPT	-	176
Al-Mg HPT	150°C 30 min	226
Al-Mg HPT	275°C 30 min	67
Al-Ti HPT	-	186
Al-Ti HPT	350°C 30 min	77
Al-Ti HPT	450°C 30 min	67

Table 2. Ultimate tensile strength and Youngs modulus of initial components in the annealed and HPT processed states.

Material / Structural state	Tensile strength σ_t, MPa	Youngs modulus *E*, GPa
Al	68	70
Al HPT	236	
Cu	190	110
Cu HPT	450	
Nb	340	155
Nb HPT	1050	
Mg	235.3	45
Mg HPT	180	
Ti	223.8	112
Ti HPT	816.3	

mainly at the interphase boundaries between different metals and at the interfaces. metals and intermetallic compounds, as can be seen in the fractography images of composite samples after tensile tests (Fig. 9).

A recent detailed analysis of the tension of a layered Al-Ti composite by *in situ* atomic tomography showed that a high level of stresses is observed at the Al/Ti interphase boundaries before the onset of tension, which grows as the tensile load appears and increases and, ultimately, lead to cracks at the interphase boundaries and the fracture of the composite [44]. To realize the compatibility of deformation and maintain the continuity of the composite, a combination of many factors is required. Obviously, at the initial (elastic) section of deformation, the components of the composite should have close values of Young's modulus, since in the opposite case, the elastic stage of deformation in a metal with a lower Young's modulus (in aluminum) ends earlier than in a metal with a large Young's modulus (in titanium) and at the next stage, the soft aluminum layers are deformed plastically, while the titanium layers, as before, are deformed only elastically, which leads to the appearance of cracks at the Al/Ti interfaces. In the Al-Mg composite, the values of the elastic moduli of Al and Mg are close (Table 2) and, apparently, no large delamination occurs at the elastic stage.

At the stage of plastic flow and hardening, it is obvious that other factors play an important role in preserving the continuity of the composite, such as the type of lattice, deformation mechanisms (slip or twinning), as well as the energy of stacking faults, reflecting the ability of dislocations to cross slip, and a number of other factors. In particular, both Mg and Ti have high stacking fault energies, the same hexagonal packed lattice, but the ratio of the lattice parameters c/a in these metals is different, in Mg $c/a > 0.63$, and in Ti $c/a < 0.63$. As a result, only one type of twinning planes operates in Mg, while in Ti the number of effective twinning planes and directions is greater and, therefore, the value of plastic deformation by twinning in Ti may turn out to be greater than in Mg. At the same time, plastic deformation during tension of the composite occurs mainly along the aluminum matrix due to multiple sliding with the formation

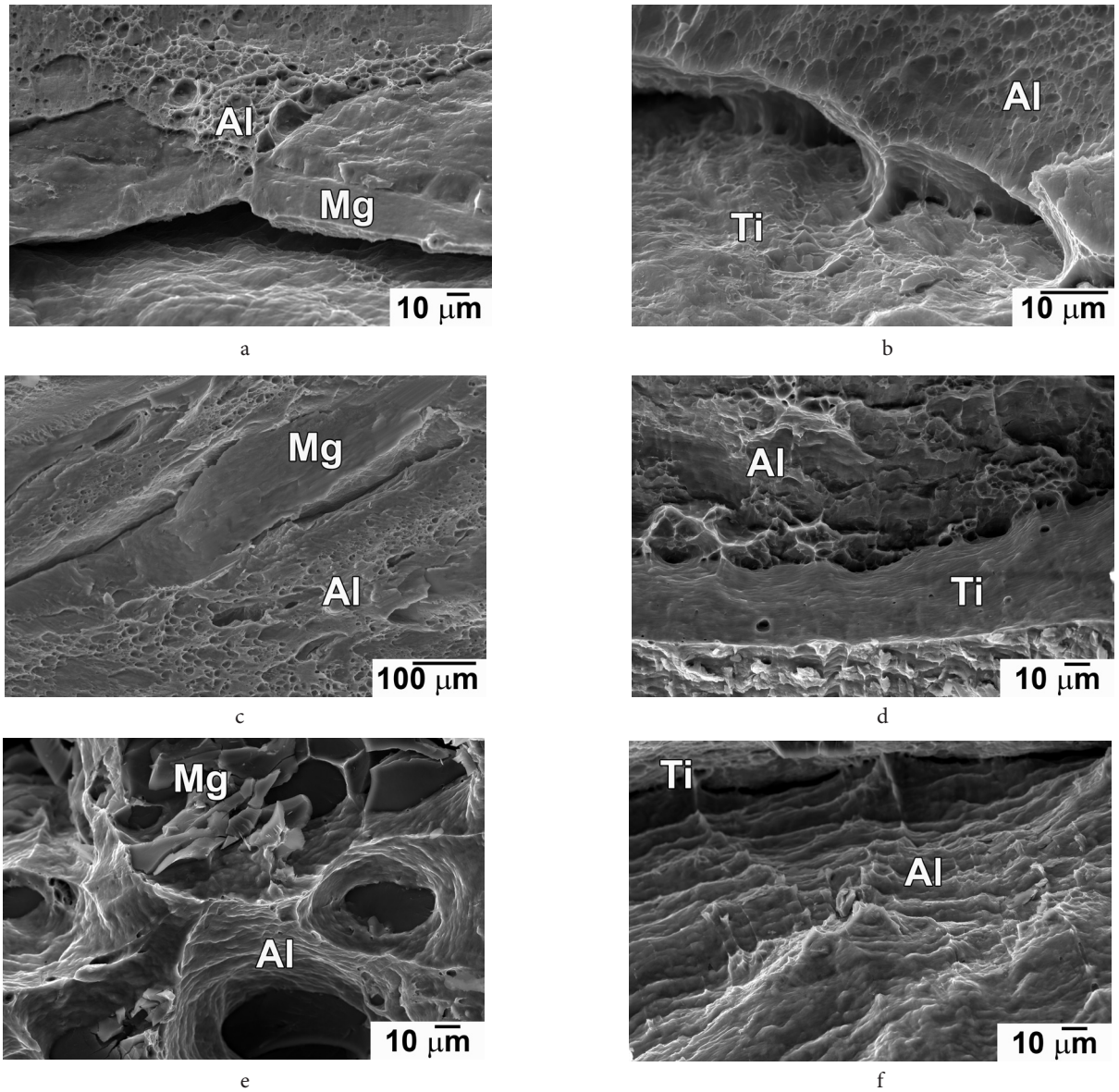

Fig. 9. Fracture surface of HPT processed hybrids Al-Mg (a, c, e) and Al-Ti (b, d, f), after tensile tests. Composites not subjected to annealing (a, b) and after annealing at 150°C (c), 350°C (d), 275°C (e), 450°C (f).

of a deep dimple fracture. In Al with an fcc lattice, the number of independent slip systems is large, which ensures the integrity of the aluminum layers during stretching. However, significant macroscopic elongation of composite specimens only due to plastic deformation of aluminum layers is practically impossible. In order for the entire sample to be deformed, it is necessary to participate in the deformation of the layers of the second components (Nb, Ti, Mg) and to relay the strain through the interphase boundaries. The presence of stresses at the interphase boundaries and delamination that appeared at the initial stages of deformation do not contribute to the joint deformation of the layers of the composites and the achievement of high strength values. As can be seen in the fracture surfaces of composites, the last points of separation are located in the aluminum phase and the obtained tensile strength values are close to those of HPT processed pure aluminum. Annealing of the composites at a relatively low temperature led, apparently, to a recovery in the aluminum matrix and to a slight increase in tensile strength; annealing of the composites at higher temperatures apparently caused grain growth and a decrease in strength to values corresponding to the strength of coarse-grained aluminum (Table 2). At the same time, the obtained values of the microhardness of composites indicate a significant strengthening of composites in comparison with pure metals. The main contribution to the hardening is made by the refinement of the grain size of the aluminum matrix (Hall-Petch hardening) and additional hardening occurs due to solid solution hardening, which, upon subsequent annealing, causes precipitation hardening.

4. Summary

In this work we have considered severe plastic deformation as a perspective method of metal matrix composites fabrication able to promote solid-state reactions through direct bonding at room temperature (RT) due to high levels of strain and pressure during the operation along with high concentration of defect during severe impacts. The structure and complex of physical and mechanical properties of the obtained composites depend on few crucial factors that we tried to address. Among few most important issues allowing to manage the material parameters one can mention the initial sample formation scheme, strain and pressure levels applied during the deformation procedure, and post deformation annealing regimes.

Final morphology and stress state of the composite sample after high-pressure torsion and subsequent annealing from the physical point of view depend on the balance between strain-induced mechanical alloying and subsequent temperature-induced precipitation.

The research performed allowed us to formulate several important conclusions presented below:

- Direct bonding of sandwich disc type sets of different metals including ones with similar lattices as Al-Cu-Al, with different lattices like Al-Mg-Al and even sets of metals with strongly dissimilar melting temperatures Al-Nb-Al, Al-Ti-Al can result in formation of bulk composites after subjecting to HPT at pressure and number of revolutions determined separately for each combination of metals. Al-Cu, Al-Nb and Al-Mg composites have similar non uniform structure. In the central regions, the low degree of mixing is observed, and the structure consists of two relatively coarse phases, with a small amount of interface boundaries. Towards the disk edges the length of interfaces increases, while the scale of the multilayered structure decreased gradually. In the case of Al-Ti the strain induced mixing on the fine level was not realized and separate coarse fragments of both components can be observed.

- HPT can induce the nucleation of the intermetallic compounds. Particles of intermetallic compositions are identified on the periphery of the Al-Cu and Al-Nb composite discs. The volume fraction of intermetallics increases monotonically along with the increase of annealing temperature. Variation of microhardness throughout the disc volume can be explained by mixing of different intermetallic phases in the annealed composite. Hard intermetallic precipitates formation, as well as Hall-Petch strengthening is responsible for the hardness increase on the composite periphery.

- Tensile tests showed a significant dependence of the tensile strength on compatibility of the deformation of the components the degree of mixing of the components. The same face centered cubic lattice of Al and Cu provides the best compatibility during tension. The tensile strength of Al-Cu hybrid was revealed to reach the level 485 MPa, which was higher than the tensile strength of both pure aluminum and copper subjected to HPT processing. This value does not obey the mixture rule due to contribution of back stresses in the transition areas to lattice dynamics during tensile tests. The main mechanism here was viscous fracture of the Al matrix without noticeable cleavage at the interphase boundaries. Annealing led to a decrease in the tensile strength due to phase transformations and precipitation of intermetallic phases at the Al/Cu interfaces. Al-Nb, Al-Mg и Al-Ti composites demonstrate ultimate tensile strength lower than initial HPT processed components due to poor deformation compatibility of layered components with different crystal lattices. The destruction in the annealed composites occurred mainly due to brittle fracture of intermetallic grains at interphase boundaries.

The results reported in this work contribute to the fundamental understanding of physical issues required for design of new approaches of metal matrix composites fabrication benefiting from both strain and hybrid configuration induced hardening.

Acknowledgments. HPT and tensile tests supported by Russian Science Foundation grant 18-12-00440-П. Energy-dispersive X-ray spectroscopy studies were performed using the equipment of the Center for Shared Access "Structural and Physicomechanical Investigations of Materials" at the Institute for Metals Superplasticity Problems, Russian Academy of Sciences. Scanning electron microscope studies supported by the program of fundamental researches and by State Task of Russian Ministry of Science and Education. EAK is grateful for financial support to the laboratory "Metals and Alloys under extreme impacts" of the Eurasian Center of Excellence.

References

1. Advanced composites in aerospace engineering. In: Advanced Composite Materials for Aerospace Engineering

(Ed. by S. Rana, R. Fangueiro.) Woodhead Publishing, Elsevier (2016) pp. 1–15. Crossref
2. T. Ishikawa, K. Amaoka, Y. Masubuchi, T. Yamamoto, A. Yamanaka, M. Arai, J. Takahashi. Compos. Sci. Tech. 155, 221 (2018). Crossref
3. N. Ralbag, J. He, D. Avnir, M. Mann-Lahav, E. S. Davydova, U. Ash, R. Galed, G. S. Grader, D. R. Dekel, M. Handl, R. Hiesgen, E. Magliocca, W. Mustain, P. Cong, A. M. Beale. Matter. 1 (4), 959 (2019). Crossref
4. B. Shi, W. Zhu, H. Yang, W. Liu, H. Tao, Z. Ling. Engineering Structures. 204, 109901 (2020). Crossref
5. Y. V. Mehr, M. R. Toroghinejad, A. Rezaeian. Mater. Sci. Eng. A. 601, 40 (2014). Crossref
6. X. Z. Wei, Q. Zhou, K. W. Xu, P. Huang, F. Wang, T. J. Lu. Mater. Sci. Eng. A. 726, 274 (2018). Crossref
7. M. O. Bodunrin, K. K. Alaneme, L. H. Chown. J. Mater. Res. Technol. 4 (4), 434 (2015). Crossref
8. D. M. Fronczek, R. Chulist, L. Litynska-Dobrzynska, S. Kac, N. Schell, Z. Kania, Z. Szulc, J. Wojewoda-Budka. Materials & Design. 130, 120 (2017). Crossref
9. A. Shyam, S. Roy, D. Shin, J. D. Poplawsky, L. F. Allard, Y. Yamamoto, J. R. Morris, B. Mazumder, J. C. Idrobo, A. Rodriguez, T. R. Watkins, J. A. Haynes. Mater. Sci. Eng. A. 765, 138279 (2019). Crossref
10. P. Shower, J. R. Morris, D. Shin, B. Radhakrishnan, L. F. Allard, A. Shyam. Materialia. 5, 100185 (2019). Crossref
11. D. Rahmatabadi, M. Tayyebi, R. Hashemi, G. Faraji. Int. J. Miner., Metall., Mater. 25 (5), 564 (2018). Crossref
12. R. Besson. Acta Materialia. 58 (2), 379 (2010). Crossref
13. M. Kawasaki, J.-K. Han, D.-H. Lee, J. Jang, T. G. Langdon. J. Mater. Res. 33 (18), 2700 (2018). Crossref
14. M. Kawasaki, J. Jang. Materials. 10 (6), 596 (2017). Crossref
15. A. Korneva, B. Straumal, R. Chulist, A. Kilmametov, P. Bała, G. Cios, N. Schell, P. Zięba. Mater. Lett. 179, 12 (2016). Crossref
16. S. O. Rogachev, S. A. Nikulin, V. M. Khatkevich, R. V. Sundeev, D. A. Kozlov. Transactions of Nonferrous Metals Society of China. 29 (8), 1689 (2019). Crossref
17. E. A. Korznikova, E. Schafler, G. Steiner, M. J. Zehetbauer. Proc. 4th Int. Symp. on Ultrafine Grained Materials, 2006 TMS Annual Meeting, TMS. Warrendale, PA (2006) p. 97.
18. W. Salgueiro, O. Garbellini, C. Morando, H. Palacio, A. Somoza. Mater. Sci. Eng. A. 435-436, 127 (2006). Crossref
19. A. P. Zhilyaev, T. G. Langdon. Progress in Materials Science. 53 (6), 893 (2008). Crossref
20. G. Korznikova, E. Korznikova, K. Nazarov, R. Shayahmetov, R. Khisamov, G. Khalikova, R. Mulyukov. Adv. Eng. Mater. 23 (1), 2000757 (2021). Crossref
21. G. Korznikova, R. Kabirov, K. Nazarov, R. Khisamov, R. Shayakhmetov, E. Korznikova, G. Khalikova, R. Mulyukov. JOM. 72 (8), 2898 (2020). Crossref
22. P. Straumal, N. Martynenko, A. Kilmametov, A. Nekrasov, B. Baretzky. Materials. 12 (18), 2980 (2019). Crossref
23. M. Liu, R. Zheng, C. Ma, N. Tsuji. Materialia. 8, 100448 (2019). Crossref
24. K. Oh-ishi, K. Edalati, H. S. Kim, K. Hono, Z. Horita. Acta Materialia. 61 (9), 3482 (2013). Crossref
25. D. Hernández-Escobar, M. Kawasaki, C. J. Boehlert. Int. Mater. Rev. (2021). Crossref
26. M. Kawasaki, J.-K. Han, S. H. Jung, J. Lee, J.-M. Park, J.-I. Jang. Adv. Eng. Mater. 22 (1), 1900483 (2020). Crossref
27. D. Hernández-Escobar, R. R. Unocic, M. Kawasaki, C. J. Boehlert. Journal of Alloys and Compounds. 831, 154891 (2020). Crossref
28. D. Hernández-Escobar, C. J. Boehlert, Z. U. Rahman, H. Yilmazer, M. Kawasaki. Philosophical Magazine. 99 (5), 557 (2019). Crossref
29. J.-K. Han, G. Y. Liang, M. Kawasaki, D. K. Han, J.-I. Jang, T. G. Langdon. Adv. Eng. Mater. 20 (11), 1800642 (2018). Crossref
30. G. F. Korznikova, K. S. Nazarov, R. Kh. Khisamov, S. N. Sergeev, R. U. Shayachmetov, G. R. Khalikova, J. A. Baimova, A. M. Glezer, R. R. Mulyukov. Mater. Lett. 253, 412 (2019). Crossref
31. R. Kulagin, Y. Beygelzimer, Yu. Ivanisenko, A. Mazilkin, B. Straumal, H. Hahn. Mater. Lett. 222, 172 (2018). Crossref
32. Y. Ru, K. Y. Yu, F. Guo, Y. Ren, L. Cui. Mater. Sci. Eng. A. 734, 77 (2018). Crossref
33. G. Korznikova, T. Czeppe, G. Khalikova, D. Gunderov, E. Korznikova, L. Litynska-Dobrzynska, M. Szlezynger. Mater. Charact. 161, 110122 (2020). Crossref
34. G. R. Khalikova, G. F. Korznikova, K. S. Nazarov, R. Kh. Khisamov, S. N. Sergeev, R. U. Shayakhmetov, E. A. Korznikova, R. R. Mulyukov. Inorganic Materials: Applied Research Variation. 12, 51409 (2021). Crossref
35. V. Tavakkoli, A. Mazilkin, T. Scherer, M. Mail, Y. Beygelzimer, B. Baretzky, Y. Estrin, R. Kulagin. Mater. Lett. 302, 130378 (2021). Crossref
36. Y. Beygelzimer, Y. Estrin, A. Mazilkin, T. Scherer, B. Baretzky, H. Hahn, R. Kulagin. Journal of Alloys and Compounds. 878, 160419 (2021). Crossref
37. H. Mostaan, F. Karimzadeh, M. H. Abbasi. Thermochimica Acta. 529, 36 (2012). Crossref
38. R. Pretorius, A. M. Vredenberg, F. W. Saris, R. De Reus. J. Appl. Phys. 70 (7), 3636 (1991). Crossref
39. X. L. Ma, C. X. Huang, W. Z. Xu, H. Zhou, X. L. Wu, Y. T. Zhu. Scr. Mater. 103, 57 (2015). Crossref
40. X. Wu, Y. Zhu. Mater. Res. Lett. 5 (8), 527 (2017). Crossref
41. X. Wu, M. Yang, F. Yuan, Y. Wei, G. Wu, X. Huang, Y. Zhu. Proceedings of the National Academy of Sciences of the United States of America. 112 (47), 14501 (2015). Crossref
42. X. Ma, C. Huang, J. Moering, M. Ruppert, H. W. Höppel, M. Göken, J. Narayan, Y. Zhu. Acta Materialia. 116, 43 (2016). Crossref
43. Y. Wang, M. Yang, X. Ma, M. Wang, K. Yin, A. Huang, C. Huang. Mater. Sci. Eng. A. 727, 113 (2018). Crossref
44. M. Huang, Ch. Xu, G. Fan, E. Maawad, W. Gan, L. Geng, F. Lin, G. Tang, H. Wu, Y. Du, D. Li, K. Miao, T. Zhang, X. Yang, Y. Xia, G. Cao, H. Kang, T. Wang, T. Xiao, H. Xie. Acta Materialia. 153, 235 (2018). Crossref